Numerical Modeling of the Thermal Behavior of Corrosion on Reinforced Concrete

Naouar LAAIDI[1], Sougrati BELATTAR[2]*
[1]Laboratory of Electronics, Instrumentation and Signal Processing
Faculty of Sciences, B.P 20. 24000 El Jadida, Morocco
naouar.laaidi@yahoo.fr
[2]Department of physics, Faculty of Sciences Semlalia, B.P. 2390, 40000 Marrakech, Morocco
*belattars@hotmail.com

Abstract. The bars in the concrete require a regular and permanent control in order to avoid the risks caused by the corrosion. In this work we present a thermal method of non destructive testing of the structures, based on numerical modeling in three dimensions. The goal is to study the detectability and the behavior of rust in the steel in transient mode by using a thermal characterization. The model of a parallelepipedic structure of concrete containing armatures of cylindrical form is adopted. This structure is supposed to be excited in the higher face by a heat flux, the lower face being maintained at constant temperature and the others faces are supposed thermically isolated.
Keyword: corrosion, rust, bars, infra-red thermography, finite elements.

1. Introduction

Defects detection and deviations in the civil engineering structures, particularly the ones containing concrete, has a very great importance in the maintenance and the prediction of the lifespan of these structures. This durability of the concrete substructures became a major subject of study during the last twenty years. Many studies have been undertaken in order to identify the suitable technique with this type of detection. Among the several techniques of non destructive testing, pulsed thermography technique proved that it's one of the best of the NDT techniques in the detection of defects located close to the surface of the considered structure [1,4] . In this paper, the modelling of pulsed thermography application in corrosion detection in steel bars is presented and analysed. This problem of corrosion represents one of the major causes of reinforced concrete structures degradation. Numerical simulations allowing better handling and variation of several parameters which have more influence on the detection of defects were adopted. Based on the finite element method, a desired model of calculating was used to describe the undertaken investigations to the level of the size and the rust depth, knowing that the rust size in the reinforcements is linked to the corrosion rate and that the modelling of the corrosion rate of these steel bars in the concrete is very important in the prediction of the lifespan of the reinforced concrete structures [5].

2. Principle of the Method

Impulse thermography is based on the active heating of structure to be investigate, by using an internal or external heat source, the idea is that heat transfer in any material is affected by a the change in its thermal properties. Indeed, the difference between temperature transient curves at surface above non defect region and above inhomogeneities is expected to include information about the defect parameters [6, 7].

In this study case one will use active infrared thermography since the reinforced concrete slab in the study do not generate heat spontaneously. The idea is to subject the structure to an external, thermal excitation, and to analyze the propagation of heat in this one. If the observed structure presents a defect, the distribution of heat inside is modified and a fine analysis of the thermogram makes it possible to highlight it.

3. Governing equations

Let us consider the following thermal equation:

$$\rho.c_p.\dot{T} - \mathrm{div}\left(\overline{\overline{\lambda}}.\overrightarrow{\mathrm{grad}T}\right) - q = 0 \qquad (1)$$

Where:

ρ : The material density

c_p : The Specific heat capacity

$\overline{\overline{\lambda}}$: The thermal tensor conductivity

q : Voluminal source of heat

With the boundary conditions:

$$\begin{cases} T = T_p \text{ on } S_T \\ \vec{n}.\overline{\overline{\lambda}}.\overrightarrow{\text{grad}T} = \varphi_S \\ S = S_T \cup S_\varphi,\ S_T \cap S_\varphi = \varnothing \end{cases} \qquad (2)$$

Where:

T_p : The imposed temperature on a surface S_T

φ_S : The imposed flow on a surface S_φ

S: The surface of the solid

$\vec{n}$: The unit vector perpendicular to S and directed towards outside

And the initial condition:

$$T(x,\ y,\ z,\ t_0) = T_0(x,\ y,\ z) \qquad (3)$$

4. Numerical modelling

The analytical resolution of the equation (1) is in general inaccessible. One is thus led to seek a solution approached by the finite element method [8, 9, 10].

The method consists in using an approximation by finite elements of the unknown functions T to discretize the variational form of the equation (1) and to transform it into system of algebric equations of the form:

$$[A]\ T = F \qquad (4)$$

Where:

A: is a square matrix of dimension [N_h, N_h]

F: is a vector of N_h components

T: is the vector of the temperatures to be calculated

We start by building the variation form of the equation (1). We carry out a spatial discretization which consists in calculating the elementary integrals by using the finite element and a temporal discretization.

There are many specialized software which make it possible to implement the method of resolution of problems by finite elements in a more or less simple and convivial way. They take care in particular of the grid of the studied object, the automatic numbering of the elements and the nodes, the calculation of a solution then of the chart of the results.

In this study, we used commercial software “Comsol” based on the finite element method and which makes it possible to calculate the evolution of temperature at any moment and in any point of material [10].

5. Description of the Studied Structure

A numerical simulation of a reinforced concrete slab (a real experience consists of a thermal heating unit, an infrared camera and a computer system which enables digital data recording in real time) is simulated. The thermal heating unit in

the experience contains three infrared radiators having a power of 2400 W each. During the infrared camera observation of the temperature distribution and the variation with time, inhomogeneities in the near surface region can be localized as far as they result in a measurable temperature difference at the surface [1,11,12,13].

The adopted parameters of numerical simulation are represented in the table below.

Input parameter	value
Material	Concrete
Size of specimen	50*50*20cm^3
Observation time including heating	4500s
Heating time	900s
Starting temperature	20 ℃
Heat density	1250 w/m^2

TableI. Input parameter for the simulation program [1,11,12]

The study concerns the influence of corrosion rate of steel bars, and the influence on concrete cover of rust. Generally, from a thermal point of view, the rust element is compared to water, since both have very close thermal characteristics [14]. When the rust attacks a cylindrical structure, the steel section decreases with the increase of corrosion layer [15], which involves a no homogeneous reduction of steel section accompanied by its embitterment and a modification of the interface physical properties (increase then reduction in adherence) [16].

When the steel reinforcement corrodes, the size of the produced rust is bigger than the size of the original steel. It increases by two or three times according to its hydration degree.

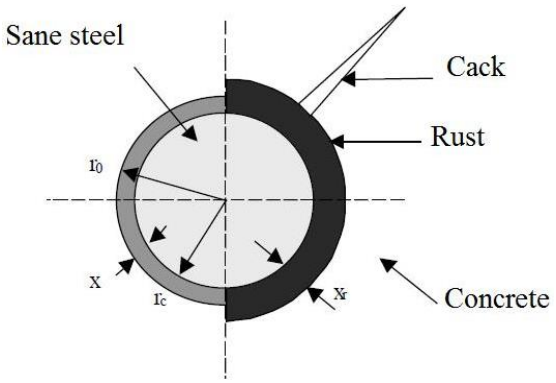

Figure 1. section of corroded steel.

x_r is the rust production, x is the corrosion depth and η is the corrosion rate. If the increase in volume is twice than the initial section, the rust production is given by the follow equation,

$$x_r = 2x \quad (5)$$

$$x_r = 2r_0(1-\sqrt{1-\eta}) \quad (6)$$

Using equations (1) and (2) [15], we can find the rust volume products for a given corrosion rate.

6. Results of Simulation

6.1. Rust Size Influence

In this study, 3 rates of corrosions were chosen, η=25%, η=50% and η=75%. For each rate of corrosion, the size of rust is determined by equation 4 and will be injected into the numerical model. A flow of 1250 w/m ^{2}is applied during 900s, for three durations during the heating, t=300s, t=600s and t=900s, and three durations during cooling t=1500s, t=3000s and t=4500s, the thermograms and the curves of evolution of temperature will be represented.

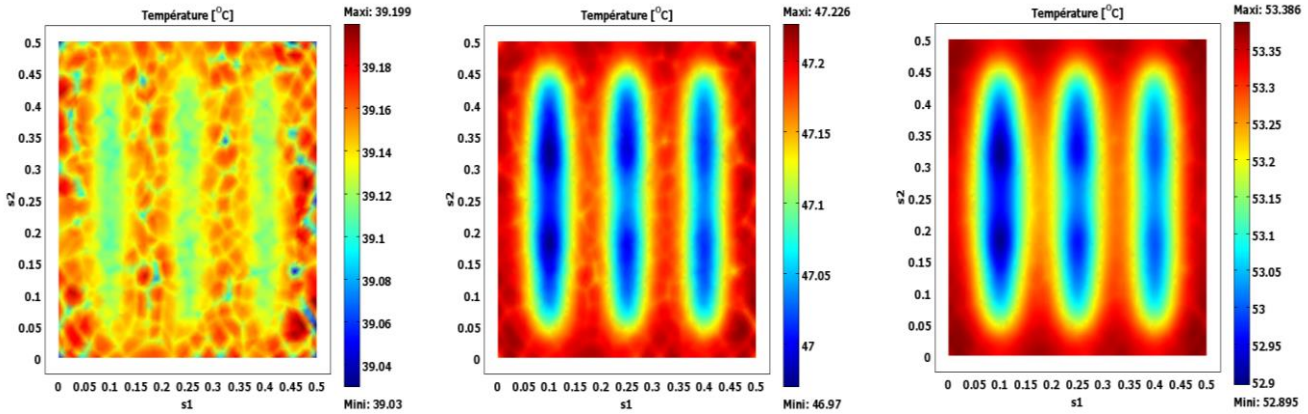

Figure 2. Recorded thermograms after a heating time of: 300s on the left, 600s on the middle and 900s on the right.

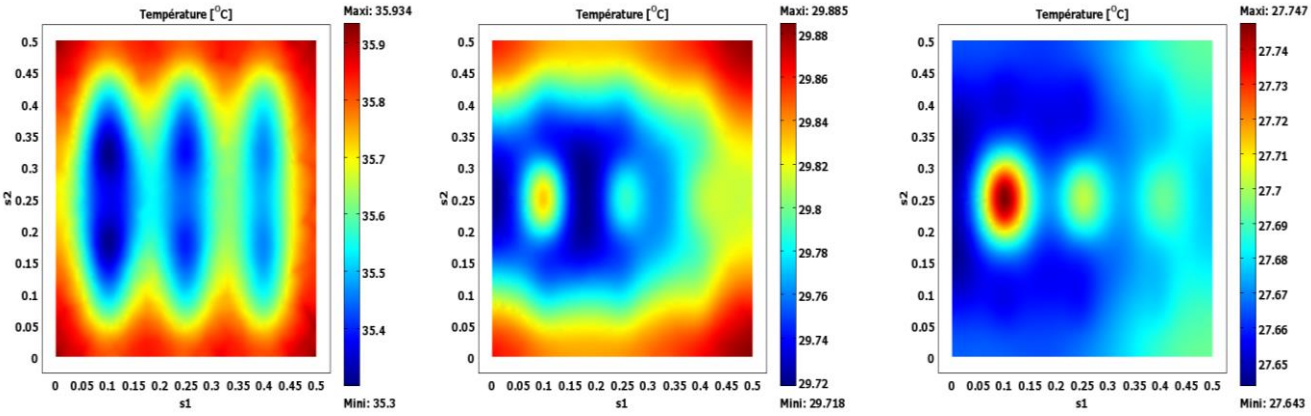

Figure 3. Recorded thermograms after a cooling down time of: 1500s on the left, 3000s on the middle and 4500s on the right.

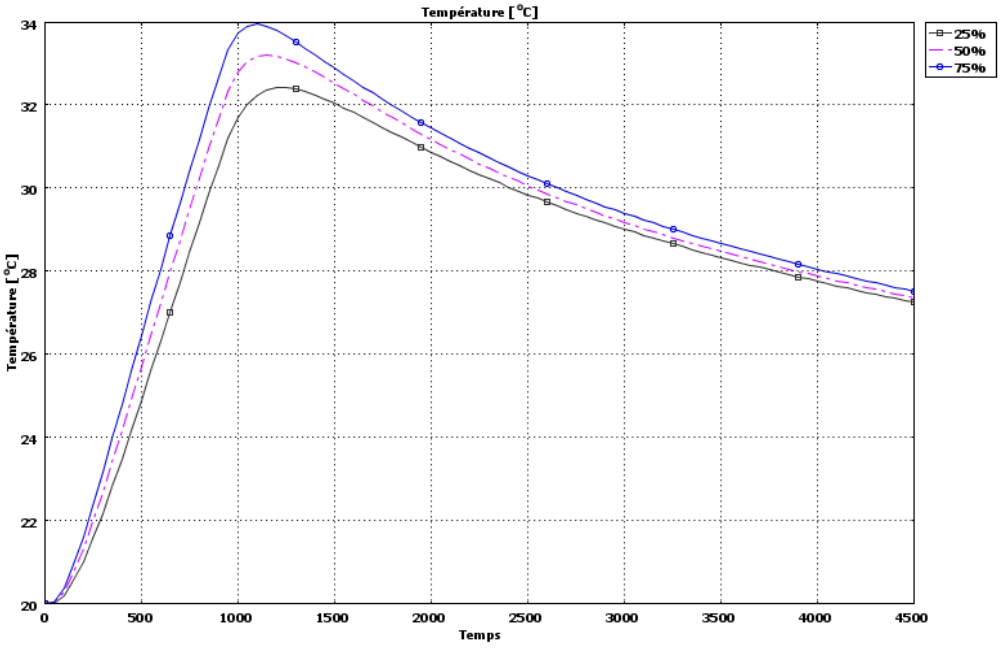

Figure 4. Temperature evolution of the rust defect for the three corrosion rates.

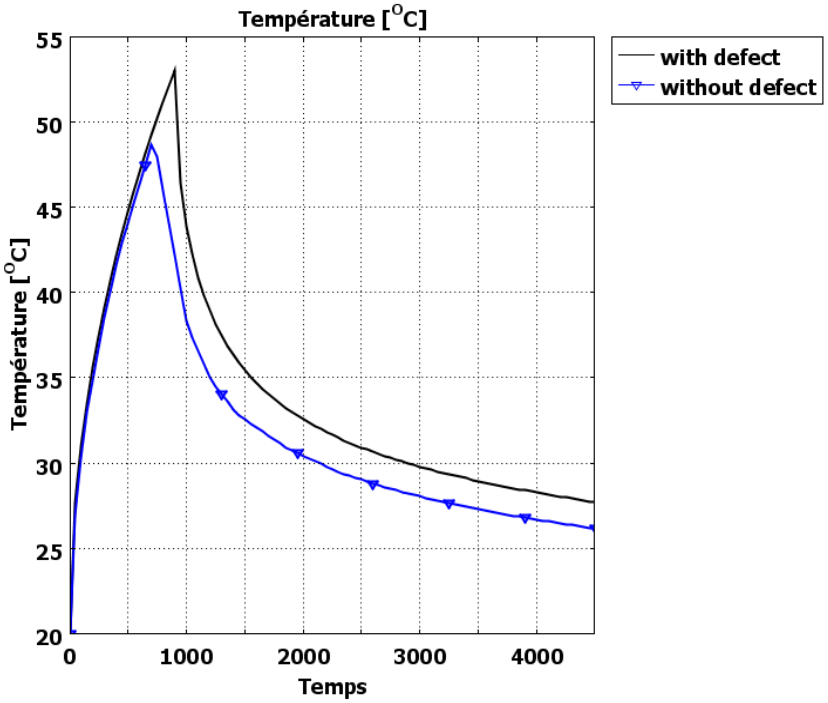

Figure 5. Temperature evolution at the surface of the concrete slab with defect compared to the case without defect.

The thermographical images of the entry face of the taken flagstone during the heating (fig.2), show that bars having a large rate of corrosion (75%) keep a less high temperature on the level of rust layers than the ones having a smaller rate of corrosion (25%), and it is due to the resistive effect of rust (k=0.6w/m.K) compared to the steel bars (k=44.5w/m.K). On the other hand, during cooling (fig.3), the most corroded bars remain hotter on the level of rust than the least corroded bars. The curves of the temperature change (fig.4) taken on the level of rust for the three corrosion rates, show that the

highest temperature corresponds to the largest rate of corrosion. Thus, the temperature taken in the center zone of the flagstone which contains the rusted bars is higher compared to that taken on the level of a flagstone without defect (fig.5). Of these remarks one can note that more the rate of corrosion increases more the detectability of rust by infra-red thermography becomes easier during the heating or cooling.

6.2. Concrete Cover Influence

In this study, for a corrosion rate of 25%, 3 positions of reinforcements were studied. A distance of 4cm between each bar was taken. A flow of 1250 w/m ^{2} is applied during 900s, for three durations during the heating, t=300s, t=600s and t=900s, and three durations during cooling t=1500s, t=3000s and t=4500s, the thermograms and the curves of evolution of temperature will be represented.

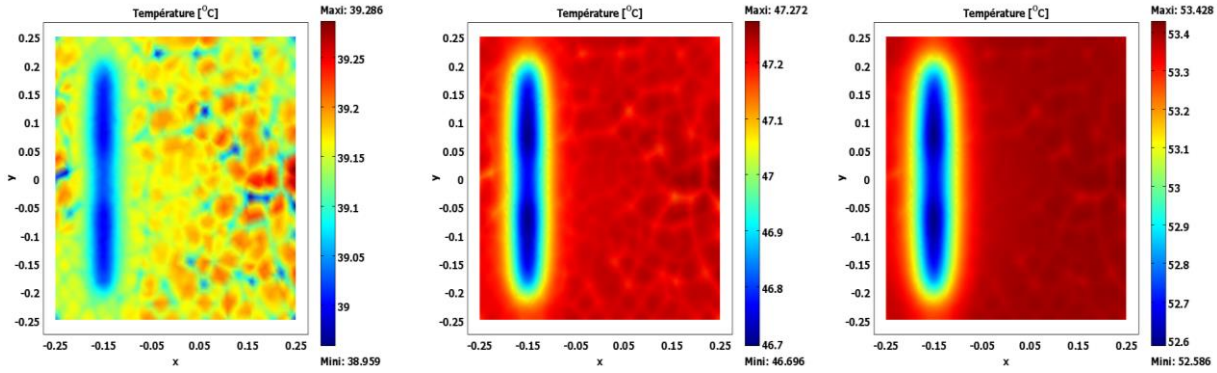

Figure 6. Recorded thermograms after a heating time of: 300s on the left, 600s on the middle and 900s on the right.

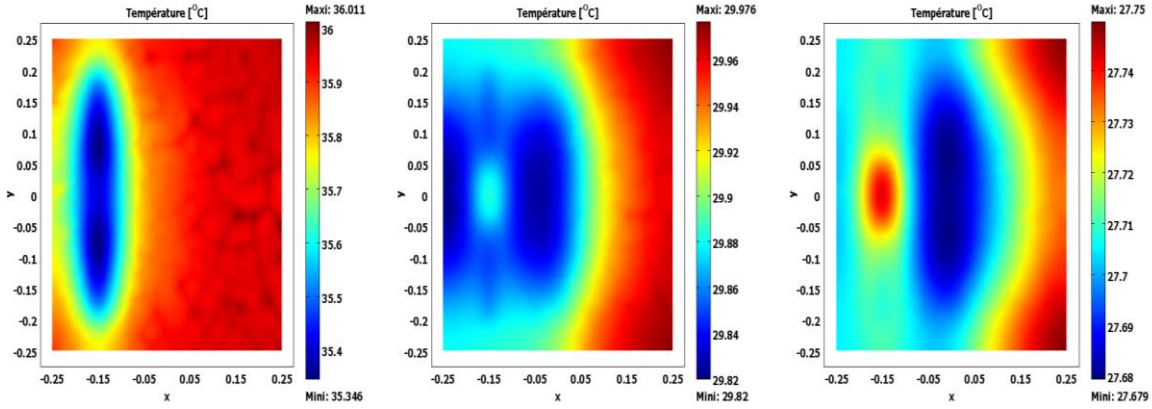

Figure 7. Recorded thermograms after a cooling down time of: 1500s on the left, 3000s on the middle and 4500s on the right.

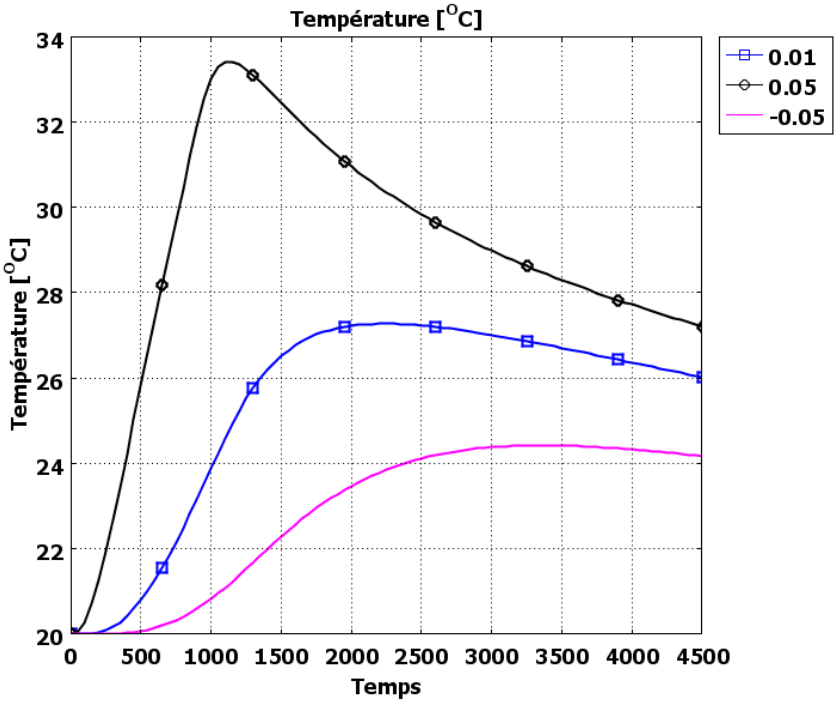

Figure 8. Temperature evolution of the rust defect for the three depths.

The thermographical images taken for the face of application of flow during the heating (fig.6) show that only the bar close to surface is detectable, however, during cooling (fig.7) the other bars appear for times of cooling much larger. The temperature taken on the level of rust for defects close to the surface is higher than that taken for bars located in bottom of the flagstone. From these remarks one can conclude that when the concrete covering becomes more important, the detection of rust is increasingly difficult.

7. Conclusion

In this study, a reinforced concrete slab containing rust defect were simulated and examined. It was noticed that the variation of the temperature at the top surface of defect and slab, depends of many parameters like the corrosion rate and the concrete cover.

As a conclusion we can note that:

- Of these remarks one can note that more the rate of corrosion increases more the detectability of rust by infra-red thermography becomes easier during the heating or cooling.
- When the concrete covering becomes more important, the detection of rust is increasingly difficult.

This study shows that the numerical methods can be used to evaluate and predict the results before beginning the experimentation; it helps to choose the suitable material to make the measures in optimal conditions and to determine when the thermal images must be taken.

References

[1] CH.Maierhofer, A.Brink, M.Rollig, H.Wiggenhausser: Transient thermography for structural investigation of concrete and composites in the near surface region. Infrared Physics & Technology 43 (2002) 271–278.

[2] CH. Maierhofer : Non-destructive testing of concrete material properties and concrete structures. Cement and Concrete Composition, 28 (2006) 297-298.

[3] CH.Maierhofer, R.Arndt, M.Rollig : Influence of concrete properties on the detection of voids with impulse-thermography. Infrared Physics & Technology 49 (2007) 213–217.

[4] D.J.Titman : Applications of thermography in non-destructive testing of structures. NDT&E International 34 (2001) 149–154.

[5] Y.Yuang, Y.Ji, J.Jiang: Effect of corrosion layer of steel bar in concrete on time-variant corrosion rate. Materials and Structures (2009) 42:1443–1450.

[6] Ch.Cheng, T.Ming Cheng, Ch.Hung Chiang: Defect detection of concrete structures using both infrared thermography and elastic waves. Automation in Construction 18 (2008) 87–92.

[7] Ch. Maierhofer, R. Arndt, M. Rollig, C. Rieck, A. Walther, H. Scheel, B. Hillemeier: Application of impulse-thermography for non-destructive assessment of concrete structures. Cement & Concrete Composites 28 (2006) 393–401.

[8] A. Elballouti, S. Belattar: Thermal non-destructive characterisation of layers detachment in the roadways. Int. J. of Materials and Product Technology, 2011, Vol. 41, No.1/2/3/4 pp. 17 - 26.

[9] N. Laaidi, S. Belattar, A. Elballouti: Pipeline Corrosion, Modeling and Analysis. J Nondestruct Eval, Volume 30, Number 3, 158-163, DOI: 10.1007/s10921-011-0103-y.

[10] Zimmerman W.B.J (2004). Process Modelling and Simulation with Finite Element Methods (World Scienti&c Series on Stability, Vibration and Control of Systems, Series A, Vol. 15. Singapore (2004).

[11] CH.Maierhofer, H.Wiggenhausser, A.Brink, M.Rollig: Quantitative numerical analysis of transient IR-experiments on buildings. Infrared Physics & Technology 46 (2004) 173–180.

[12] CH.Maierhofer, A.Brink, M.Rollig, H.Wiggenhausser: Quantitative impulse-thermography as non-destructive testing method in civil engineering – Experimental results and numerical simulations. Construction and Building Materials 19 (2005) 731–737.

[13] Ch. Maierhofer, R. Arndt, M. Rollig, C. Rieck, A. Walther, H. Scheel, B. Hillemeier: Application of impulse-thermography for non-destructive assessment of concrete structures. Cement & Concrete Composites 28 (2006) 393–401.

[14] F.J. Molina, C. Alonso, C. Andrade: Cover cracking as a function of rebar corrosion. Part 2 - Numerical model. Materials and Structures, 1993, 26, 532-548.

[15] M. Dekoster, O. Blanpain, F. Buyle-Bodin, O. Maurel : Etude de l'évolution des coefficients de sécurité des ouvrages en béton armé dégradé selon différents scénarios de corrosion. XXIIiemes Rencontres Universitaires de Génie Civil 2004 - Ville & Genie civil.

[16] Q. T. Nguyen, S. Caré, Y. Berthaud, A. Millard: Analyse de la fissuration du béton armé en corrosion accélérée. C. R. Mecanique 335 (2007) 99–104.